

Mini-band states in graded periodic 1D photonic superstructure

C.-F. Ying · W.-Y. Zhou · Q. Ye · Z.-B. Li · J.-G. Tian

Received: 19 June 2011 / Revised version: 12 January 2012 / Published online: 21 March 2012
© Springer-Verlag 2012

Abstract The shallow mini-band states have been clearly located in experiment in the graded periodic structure which was fabricated by the holography method. We demonstrated that the band edge folding and splitting into individual shallow levels are due to long-periodic modulation. Numerical simulations show strong slow-light effect and low second-order dispersion of mini bands. By taking into account the non-uniform distribution of the material, the numerical results agree quite well with the experimental results. To our knowledge, this is the first instance in which shallow mini-band states have been experimentally located in a graded periodic film via the holography method.

1 Introduction

As we know well, semiconductors form the basis of all electronics' applications. Photonic crystals (PCs), the optical analogues of electronic semiconductors, are considered as the next potential revolution of the information technology and are attracting more and more researchers. Among the researches on PCs, many previous studies have been focused on the manipulation of group velocity. Recently, the "slow-light" effect in PCs [1] has attracted a great deal of interest in practical applications, such as low-threshold lasing [2–4], pulse delay [5, 6], and enhanced nonlinear in-

teractions [7, 8]. Generally, the defects in photonic crystals [9–11] or periodically positioned structural defects in coupled resonator optical waveguides (CROWs) [12, 13] can support localized modes and these localized modes in the cutoff wavelengths can strongly modify the group velocity in the vicinity. However, the fabrication of specific type of defects at specific location within PCs is not so straightforward. Previous works on the CROWs were mainly focused on theory and numerical simulation.

Another way to control the formation of states within the forbidden gap is optical superlattice. There are narrow bands with low dispersion induced by the bandgap folding in an optical superlattice. These induce low group velocity and high density of states. Furthermore, these researches of narrow bands have been experimentally realized in several superlattices such as optical fiber gratings [14], colloidal photonic superlattices [15, 16], and superstructure surface plasmons [17, 18]. Several theoretical researches have been carried out for the slow light in the dual-periodic crystals [19, 20], which were focused on the EM field enhancement in a particular spatial region. For examples, the energy is confined in the vicinity of every π shift region in moiré grating. Ymilov et al. [21] have reported the dual-periodic photonic crystals formed by four *s*-polarized laser beams theoretically. In this structure, the EM field is localized in the whole multilayer regions. In other words, the active materials can be excited in larger region, which provides further applications over the excitation and nonlinearity enhancement. However, an experimental fabrication of holographic superstructure in thin film has not been reported, yet.

This paper presents the fabrication of photonic superstructure by four-beam interference holography on dichromated gelatin (DCG) emulsion. Experimental transmission spectra with three or four distinct mini bands between the forbidden gaps were presented. By taking into account the

C.-F. Ying · W.-Y. Zhou (✉) · Q. Ye · Z.-B. Li · J.-G. Tian
School of Physics, Nankai University, Tianjin 300071, China
e-mail: wyzhou@nankai.edu.cn
Fax: +86-022-23508379

Z.-B. Li · J.-G. Tian
The Key Laboratory of Weak Light Nonlinear Photonics, Ministry of Education, Teda Applied Physics School, Nankai University, Tianjin 300457, China

non-uniform correction and surface grating of the structure, the numerical analysis for transmission spectra is in good agreement with our experimental data. The mini bands can be seen as band-edge states folding and split off into shallow levels by the long-period modulation. Furthermore, results show that strong slow-light effect can exit in the mini-band states of low second order dispersion, and the EM field is confined in the whole multilayer regions. To our knowl-

edge, this is the first instance in which shallow mini-band states have been experimentally located in a graded periodic film via the holography method.

2 Experimental

The recording plates were prepared similar to that reported earlier in [22]. The photosensitive solution, by mixing 4.4 % gelatin and 0.72 % ammonium dichromate with 94.88 % distilled water, was spread to a glass plate in a darkroom and the thickness of dry film was about 20 μm . A general experimental configuration of 1D superstructure formed by four-beam interference holography in DCG emulsion is shown in Fig. 1. Two coherent *s*-polarized beams with wavelength 488 nm and power ratio of 59:41 are incident on the emulsion. The diameters of two beams are 20 mm and the incident angles are about $65^\circ \pm 3^\circ$, respectively. The gelatin side was doped in the index-matching liquid (dimethylbenzene). Under the liquid was a silver mirror. After exposure, the DCG plate was dipped in 20 % Kodak Rapid Fixer. Then the plate was soaked in distilled water for 15 min. After the soaking step it was dehydrated respectively in 50 %, 75 %, 95 %, and 100 % isopropyl alcohol. Finally, the DCG plate was dried in the oven at 40 $^\circ\text{C}$.

Figure 2(a)–(d) shows the transmission spectra of the superstructure (sample *a*–*d*) fabricated by four-beam interference. The optical transmission spectra were measured with a fiber spectrometer (Ocean Optics, HR4000). A collimated

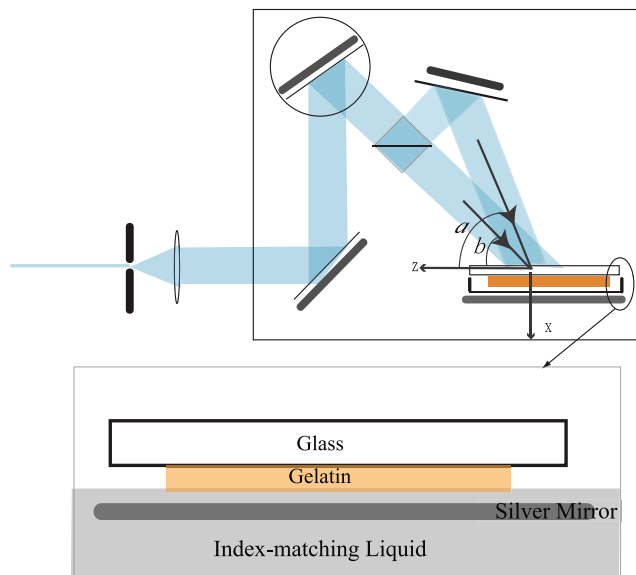


Fig. 1 Schematic diagram of the optical layout for the experimental configuration

Fig. 2 (a)–(d) are the transmission spectra of four samples. (e) The AFM image of the DCG emulsion surface. The *inset* is the spatial distribution of energy along the *z* direction at normal incidence. (f) Distribution of the refractive index inside the sample *d*

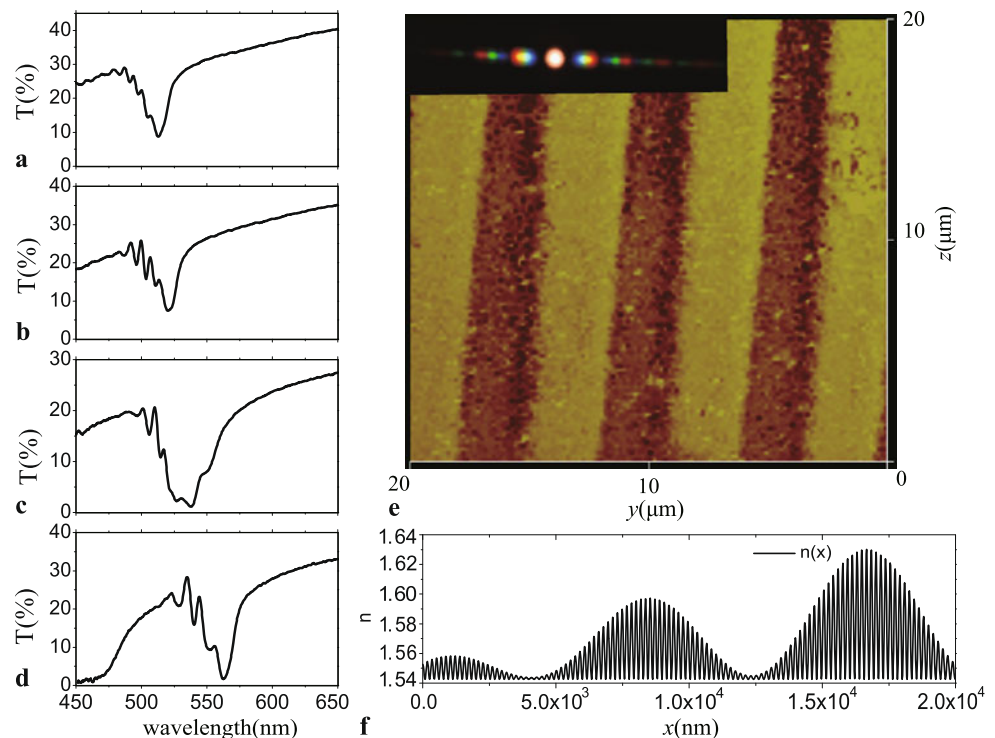
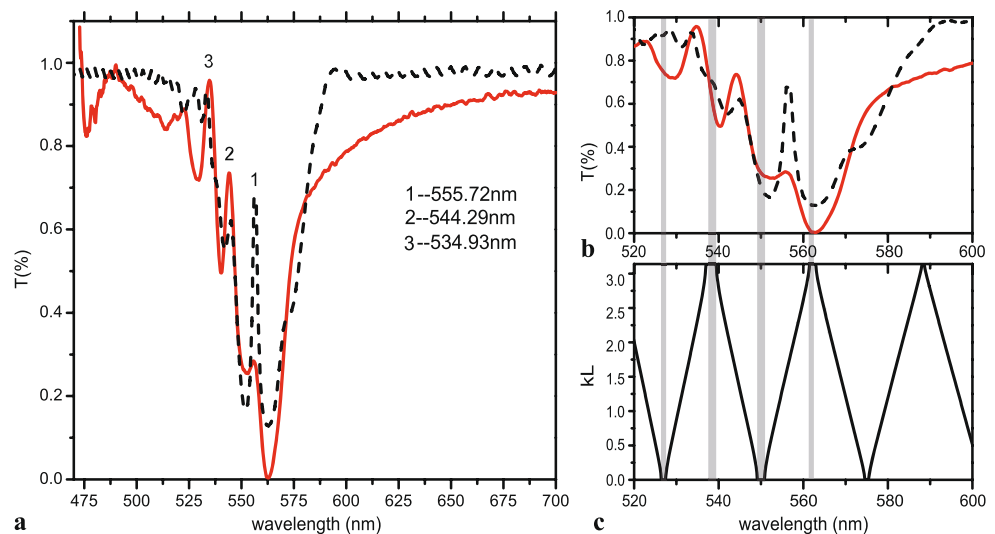


Fig. 3 (a) The normalized experimental transmission spectra (red solid curve) and numerical result (black dashed curve) under normal incidence. (b) Transmission spectra of the structure with wavelength of 520 to 600 nm. (c) Photonic band structure in the first Brillouin zone for superstructure as an infinite number of layers stacking along the x -axis direction



beam from tungsten–bromine lamp with a diameter of 5 mm was used as white light source. There are three or four distinct mini bands within the forbidden gap in each sample (Fig. 2(a)–(d)). Four-beam interference pattern can form a surface grating on x – y surface, which leads to the spatial distribution of energy, as shown in the inset of Fig. 2(e). Therefore, there is about 30 % of transmission energy in the zero order. Fig. 2(e) is the atomic force microscopy (AFM) image of the emulsion surface of sample d , the periodic of grating is about 5.7 μm , from which we can get the incidence angles $a = 63.4^\circ$ and $b = 68.5^\circ$, precisely.

3 Theoretical analysis and discussion

The dielectric function formed by interference photolithography method can be written in the form

$$n = n_0 + \Delta n [\alpha \cos(k_1 x) + \beta \cos(k_2 x)]^2, \quad \alpha + \beta = 1. \quad (1)$$

Here n_0 is the bulk refractive index, Δn is the maximum refractive index change of the material. $k_1 = K_0 \sin(a)$, $k_2 = K_0 \sin(b)$, where K_0 is the wave vector of writing beam in vacuum. $\alpha:\beta$ is the ratio of energy of two beams. The refractive index is modulated by two spatial periods: the slowly varying period $L = 2\pi/(|k_1 - k_2|)$ and the rapidly varying period $l = 2\pi/(k_1 + k_2)$. The Bragg frequency is determined by the rapidly varying frequency $\omega_B = \pi/n_0 l$. The long-period modulation can induce band edge folding in the Brillouin zone and leads to the mini bands which can be seen as band-edge states split off.

In our experiment, the structure of the DCG PCs is not strictly periodic because of the absorption and development process [23, 24]. They lead to gradually-varied amplitude and spatial frequency of the $n(x)$. To further analyze these three mini bands, numerical simulated transmission spectra

by taking into account the non-uniform of DCG was calculated to match the measured curves. The amplitude and spatial frequency of $n(x)$ are given by

$$\Delta n(x) = \Delta n(0) [(1 - p)^r + p], \quad (2)$$

$$K = K(0) - \Delta K \frac{x}{T}. \quad (3)$$

$\Delta n(0)$ and $K(0)$ are the amplitude and spatial frequency of refractive index in the air–gelatin interface, respectively. T is the thickness of the emulsion. We get parameters of sample d : $p = 0.1$, $r = 0.8$, $\Delta K = 0.0152 \times K(0)$. Substituting Eqs. (2) and (3) into Eq. (1), Fig. 2(f) shows the distribution of the refractive index modulation by taking into account the non-uniform of DCG.

We consider that a plane wave is incident normally on a multilayer structure in an air background. The wave propagates along the x direction. The EM fields within different layers can be connected to each other with a transfer matrix by which Maxwell's equations are solved within every single layer. The transfer matrix for a long period can be expressed as

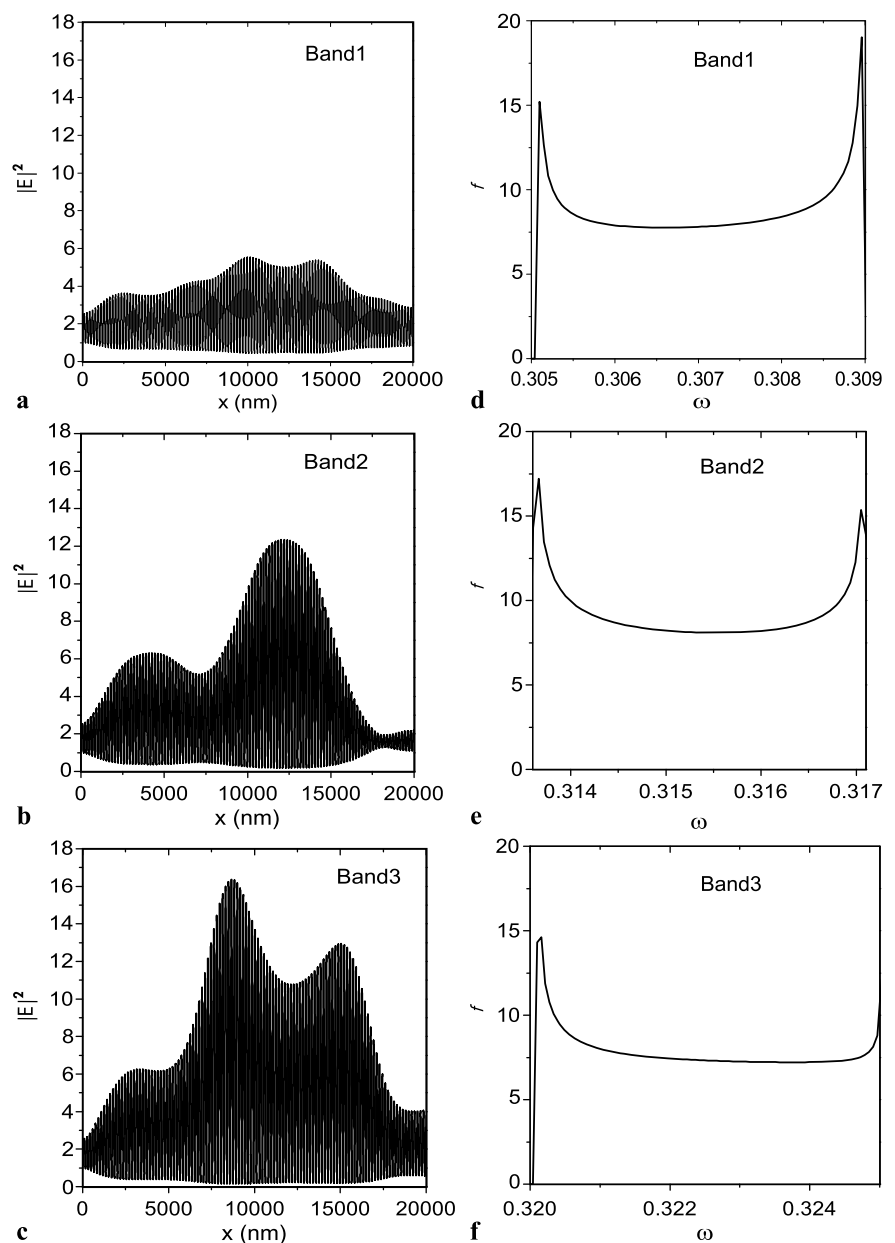
$$M = \begin{bmatrix} m_{11} & m_{12} \\ m_{21} & m_{22} \end{bmatrix}. \quad (4)$$

According to Bloch's theorem, one can easily obtain the dispersion relation for the superstructure under normal incidence conditions.

$$\cos(\mathbf{k}L) = \frac{m_{11} + m_{22}}{2}. \quad (5)$$

In the Brillouin zone, the back scattering light has the same phase as the forward light, which interference to be a standing wave, and the group velocity is zero. Because the slow light mode is the resonant mode of the lattice, the slow-light mode can be controlled by adjusting the geometrical parameters of the PC structure. If the Brillouin zone was compressed by the long-period modulation, the band-edge

Fig. 4 (a)–(c) Electric field intensity ($|E|^2$) inside the uniform sample when a plane wave with center frequency of each mini bands is incident upon it. (d)–(f) Localized factors of the three bands



modes folding into series of bands, and the interference between back scattering light and forward light induce them split off into mini bands. Some of these bands correspond to as sharp peaks in the forbidden gap region in transmission spectra.

Below, we discuss sample *d* formed by four-beam interference in our experiment. The refractive index as a function of *x*-axis is shown in Fig. 2(f). The bulk refractive index $n_0 = 1.5426$, and the maximum refractive index change of the material $\Delta n = 0.1$. Considering the loss of the transmission energy induced by the surface grating, the transmission spectra are normalized. After the TMM calculation, one can see in Fig. 3(a) that the simulated result agrees well with measured ones within the transmission gap. There are three

distinct transmission mini bands between the forbidden gaps and the band-width of each mini band is about 5 nm. The *Q* factors ($Q = \omega_0/\Delta\omega$, ω_0 is the center frequency of mini bands) of each resonator for the center wavelength of $\lambda_1 = 555.72$ nm, $\lambda_2 = 544.29$ nm, and $\lambda_3 = 534.93$ nm are $Q_1 = 55$, $Q_2 = 120.5$, and $Q_3 = 103$, respectively, which were obtained by Gauss fitting of the measured curves. The great agreement between the numerical simulation and experimental result provides convincing evidence that the observed mini bands arise indeed from superstructure effect. Figure 3(c) is the photonic band structure of the superstructure calculated by the TMM. There are three bands between four forbidden gaps.

Let's discuss some details of these mini bands. The dispersion of group velocity can be expanded in Taylor series

$$K(\omega) = \beta_0 + \beta_1(\omega - \omega_0) + \frac{\beta_2}{2}(\omega - \omega_0)^2 + \frac{\beta_3}{6}(\omega - \omega_0)^3 + \dots, \quad (6)$$

$$\beta_1 = \frac{c}{v_g} = \left(\frac{dk'}{d\omega} \right)_{\omega=\omega_0}, \quad (7)$$

where β_1 , β_2 , and β_3 are the one, two and three-order dispersion expand coefficients of the group velocity, respectively, c is the speed of light in vacuum, and $k' = ka/2\pi$ is the normalized wave vector. The localized factor can be defined as

$$f = \sqrt{\frac{v_g^{\text{bulk}}}{v_g^{\text{PC}}}} = \sqrt{\frac{1}{n_0}} \sqrt{\beta_1}. \quad (8)$$

f denotes the electro-magnetic field localization ability of resonators. From the Eqs. (5), (7) and (8), the localized factor turns out to be functions of the transfer matrix M for one super periodic of uniform grating. The localized factors f versus frequency for three bands is shown in Fig. 4(d)–(f). Within the center frequency of each band, f is almost constant, which indicates low second order dispersion of group velocity in the band. Therefore, these mini bands have weak distortion in pulse signal and have advantages in information processing applications. The field distributions within the superstructure for three bands with center frequencies of $\omega_1 = 0.307$, $\omega_2 = 0.3153$, $\omega_3 = 0.3225$ are given in Fig. 4(a)–(c). For the center frequency of band-1 and band-3, the energy is localized at the peak region of $n(x)$ in a super cell, but at the valleys of $n(x)$ for the center frequency of band-2.

The valleys and peaks region of $n(x)$ can be regarded as resonators in which the EM field can be confined. Photons can be localized within these regions by multiple reflections when the specific condition is satisfied. The long-period refractive index modulation creates periodic spatial bending which can be separated the resonators by the tunneling barriers. The mini bands with slow light effect are created due to the interaction between the resonators via weak coupling across tunneling barriers like the CROWs. Therefore, one can expect the electric field intensity $|E|^2$ to be increased considerably in the localized regions for specific narrow band mode. In application to the nonlinearity and fluorescence excitation, enhancement intensity in large region would provide larger active region.

4 Conclusion

In this work, we present a large-area and high-quantity fabrication method of 1D photonic superstructure in gelatin

emulsion using the four-beam interference technique. Experimental transmission spectra exhibit obvious mini bands in the forbidden gap. The electric intensity is localized in the whole multilayer region within the center frequency of mini bands. This is the first time mini bands were observed in non-uniform film via holographic method. Based on TMM and non-uniform correction, numerical simulations of transmission spectra agree well with the experimental results. Result shows that the mini bands have strong slow-light effect and weak second order dispersion of group velocity. Because of the advantages of DCG, the superstructure has potential in application of holographic crystals. Meanwhile, unlike the CROWs and other superlattices, the electromagnetic field was enhanced in the whole region of multilayer structure and the active materials can be excited in larger region. A study on the application of excitation and nonlinearity enhancement in this superstructure will be carried out in our further work.

Acknowledgements This research is supported by the Chinese National Key Basic Research Special Fund (No 2011CB922003), the National Key Basic Research and Development Program of China under Grant (No 2010CB327605), Chinese Natural Science Foundation (No 11174162), Tianjin Natural Science Foundation (No 09JCYBJC01600), Science and Technology Program of Tianjin (No 10ZCGHHZ01100), and Fundamental Research Funds for the Central Universities (No 65010931).

References

1. T. Baba, Nat. Photonics **2**, 465 (2008)
2. J.P. Dowling, M. Scalora, M.J. Bloemer, C.M. Bowden, J. Appl. Phys. **75**, 3 (1994)
3. V.I. Kopp, Opt. Lett. **23**, 1707 (1998)
4. B.M. Shkunov, Z.V. Vardeny, M.C. Delong, R.C. Polson, A.A. Zakhidov, R.H. Baughman, Adv. Funct. Mater. **12**, 21 (2002)
5. K. Yoshino, S. Tatsuhara, Y. Kawagishi, M. Ozaki, Appl. Phys. Lett. **74**, 2590 (1999)
6. D. Mori, T. Baba, Appl. Phys. Lett. **85**, 1101 (2004)
7. S. Chen, W. Zang, A. Schülzgen, X. Liu, J. Tian, J.V. Moloney, N. Peyghambarian, Opt. Lett. **34**, 3665 (2009)
8. J.D. Joannopoulos, Nat. Mater. **3**, 211 (2004)
9. P. Tran, J. Opt. Soc. Am. B **14**, 2589 (1997)
10. M. Notomi, K. Yamada, A. Shinya, J. Takahashi, C. Takahashi, I. Yokohama, Phys. Rev. Lett. **87**, 253902 (2001)
11. X. Liu, S. Chen, W. Zang, J. Tian, Opt. Express **19**, 8233 (2011)
12. J.K. Poon, J. Scheuer, Y. Xu, A. Yariv, J. Opt. Soc. Am. B **21**, 1665 (2004)
13. A. Yariv, Y. Xu, R.K. Lee, A. Scherer, Opt. Lett. **24**, 711 (1999)
14. H. Ishii, H. Tanobe, F. Kano, Y. Tohmori, Y. Kondo, Y. Yoshikuni, IEEE J. Quantum Electron. **32**, 433 (1996)
15. K. Baert, K. Song, R.A. Vallée, M.V. Auweraer, K. Clays, J. Appl. Phys. **100**, 123112 (2006)
16. R. Rengarajan, P. Jiang, D.C. Larrabee, V.L. Colvin, D.M. Mittleman, Phys. Rev. B **64**, 205103 (2001)
17. A. Kocabas, S.S. Senlik, A. Aydinli, Phys. Rev. Lett. **102**, 063901 (2009)

18. S. Balci, M. Karabiyik, A. Kocabas, *Plasmonics* **5**, 429 (2010)
19. D. Janner, G. Galzerano, G.D. Valle, P. Laporta, S. Longhi, M. Belmonte, *Phys. Rev. E* **72**, 056605 (2005)
20. R. Shimada, T. Koda, T. Ueta, K. Ohtaka, *J. Appl. Phys.* **90**, 3905 (2001)
21. A.G. Yamilov, M.F. Bertino, *Opt. Lett.* **32**, 283 (2007)
22. C. Ying, W. Zhou, Q. Ye, X. Zhang, *J. Opt.* **12**, 115101 (2010)
23. Z. Ren, T.R. Zhai, Z.N. Wang, J. Zhou, D. Liu, *Adv. Mater.* **20**, 2337 (2008)
24. R. Ma, J. Xu, W. Yim, *Appl. Phys. Lett.* **89**, 081116 (2006)